A mitochondrial uncoupling artifact can be caused by expression of uncoupling protein 1 in yeast

Jeff A. STUART*†, James A. HARPER*†, Kevin M. BRINDLE†, Mika B. JEKABSONS* and Martin D. BRAND*[1]

*MRC Dunn Human Nutrition Unit, Hills Road, Cambridge CB2 2XY, U.K., and †Department of Biochemistry, University of Cambridge, Tennis Court Road, Cambridge CB2 1GA, U.K.

Uncoupling protein 1 (UCP1) from mouse was expressed in yeast and the specific (GDP-inhibitable) and artifactual (GDP-insensitive) effects on mitochondrial uncoupling were assessed. UCP1 provides a GDP-inhibitable model system to help interpret the uncoupling effects of high expression in yeast of other members of the mitochondrial carrier protein family, such as the UCP1 homologues UCP2 and UCP3. Yeast expressing UCP1 at modest levels (approx. 1 μg/mg of mitochondrial protein) showed no growth defect, normal rates of chemically uncoupled respiration and an increased non-phosphorylating proton conductance that was completely GDP-sensitive. The catalytic-centre activity of UCP1 in these yeast mitochondria was similar to that in mammalian brown-adipose-tissue mitochondria. However, yeast expressing UCP1 at higher levels (approx. 11 μg/mg of mitochondrial protein) showed a growth defect. Their mitochondria had depressed chemically uncoupled respiration rates and an increased proton conductance that was partly GDP-insensitive. Thus, although UCP1 shows native behaviour at modest levels of expression in yeast, higher levels (or rates) of expression can lead to an uncoupling that is not a physiological property of the native protein and is therefore artifactual. This observation might be important in the interpretation of results from experiments in which the functions of UCP1 homologues are verified by their ability to uncouple yeast mitochondria.

Key words: mitochondria, proton leak, uncoupling protein 1.

INTRODUCTION

Uncoupling protein 1 (UCP1) is present in the inner membrane of brown-adipose-tissue mitochondria, in which it catalyses a regulated proton conductance that leads to an uncoupling of oxidative phosphorylation and non-shivering thermogenesis [1]. UCP2 and UCP3 are close homologues of UCP1 that have been proposed to uncouple oxidative phosphorylation in other tissues [2–4]. Other members of the mitochondrial carrier protein family with weaker sequence similarity to UCP1 {plant UCP 'PUMP' and stUCP [5,6], UCP4 [7] and brain mitochondrial carrier protein 1 ('BMCP1') [8]} have also been implicated in uncoupling.

There is debate over whether these homologues of UCP1 naturally catalyse proton conductance and over what physiological relevance such uncoupling might have [1,9–11]. The main evidence in favour is that they are able to uncouple oxidative phosphorylation when they are expressed in yeast [2,12–15] and when they are overexpressed in transgenic mice [16,17]. Other evidence comes from muscle mitochondria from UCP3 knock-out mice, which are reported to be better coupled and have lower proton conductance than controls [18,19], and from UCP2 and UCP3 reconstituted into proteoliposomes, which are associated with increased conductance of chloride ions and protons [20,21].

However, physiological increases in mammalian UCP2 or UCP3 expression are not associated with increased uncoupling [9–11]. In starved rats, muscle UCP3 mRNA levels increase but muscle thermogenesis declines [22], and mitochondrial UCP3 protein content doubles but no increase in proton conductance is observed [23]. In hyperthyroid rats, UCP2 and UCP3 mRNA levels increase but (when non-esterified fatty acid concentrations are standardized between treatments) no differences in mitochondrial uncoupling are apparent [24,25]. In UCP1 knock-out mice, brown-adipose-tissue UCP2 mRNA increases 14-fold but proton conductance remains the same [26]. In mice treated with lipopolysaccharide, UCP mRNA levels change over time in liver and skeletal muscle but mitochondrial proton conductance does not [27]. Similarly, there is no correlation between tissue and species expression of UCP2 and UCP3, and the observed basal uncoupling of mitochondrial respiration [9,10].

Thus it is reasonable to ask whether the uncoupling phenotype observed in the genetically altered model systems represents a native activity of the UCP1 homologues or an artifact of compromised mitochondrial integrity that causes an uncoupling that is not a normal function of the native protein. This possibility has been recognized previously [8,14] but has not been tested rigorously. Here we use UCP1 expressed in yeast as a model to assess the yeast heterologous expression systems commonly used to demonstrate uncoupling by the homologues of UCP1. The native proton conductance of UCP1 can be activated by palmitate and completely inhibited by purine nucleotides such as GDP, allowing us to distinguish unambiguously between the effects of protein activity itself and the non-specific effects of manipulating expression levels. We show that modest UCP1 expression in yeast results in native UCP1 activity but that higher UCP1 expression can indeed result in mitochondrial uncoupling that is not GDP-sensitive and hence is not a native function of UCP1. An abstract of this work has been published previously [28].

EXPERIMENTAL

Expression of UCP1 in *Escherichia coli*

Mouse UCP1 (mUCP1) expressed in *E. coli* and accumulated as inclusion bodies was used to calibrate the UCP1 content of yeast mitochondria. A PCR product for mUCP1 (see below) was

Abbreviations used: mUCP1, mouse UCP1; TMPD, *N,N,N′,N′*-tetramethyl-*p*-phenylenediamine; TPMP, methyltriphenylphosphonium; UCP, uncoupling protein.

[1] To whom correspondence should be addressed (e-mail martin.brand@mrc-dunn.cam.ac.uk).

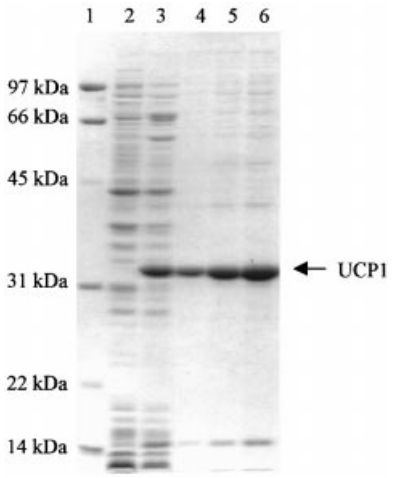

Figure 1 Coomassie-stained SDS/PAGE gel showing the expression of UCP1 in *E. coli* and its partial purification by the isolation of inclusion bodies

Lane 1, molecular mass markers (molecular masses indicated at the left); lane 2, homogenate of *E. coli* empty vector after 2 h of induction (20 μg of protein); lane 3, homogenate of *E. coli* with pET-UCP1 homogenate after 2 h of induction (20 μg of protein); lanes 4, 5 and 6, solubilized UCP1 inclusion bodies isolated from *E. coli* after 2 h of induction loaded at 5, 10 and 15 μg of protein respectively.

modified to incorporate a silent A → C substitution at position 582 in the coding sequence to eliminate an internal *Nde*I site, then ligated into *Nde*I and *Eco*RI restriction sites of the pET expression vector pMW172 [29]. Competent C41 (DE3) strain *E. coli* were transfected with either pET-mUCP1 or empty pET vector. Cultures were incubated in TB medium with 100 μg/ml ampicillin at 37 °C at 250 rev./min until D_{600} reached 0.5–0.6. Expression was induced with 1 mM isopropyl β-D-thiogalactoside. After 2 h, cells were harvested by centrifugation at 3000 ***g*** for 15 min. All centrifugation steps were performed at 4 °C. Cell pellets were stored at −85 °C.

Cells were lysed in B-PER reagent (Pierce) for 10–15 min at room temperature, centrifuged at 27200 ***g*** for 15 min and resuspended in B-PER containing 200 μg/ml lysozyme for 5–10 min to lyse any remaining cells. Inclusion bodies were harvested by centrifugation at 27200 ***g*** for 15 min. The pellet was washed three times by resuspension in buffer containing 150 mM potassium phosphate, 25 mM EDTA, 1 mM dithiothreitol, 1 mM ATP, pH 7.8 [20], and centrifugation at 27200 ***g***. The final pellet was solubilized in 1.5% (w/v) *N*-laurylsarcosine for 45 min at room temperature. Insoluble material was removed by centrifugation at 27200 ***g*** for 15 min. The supernatant ('solubilized UCP1 inclusion bodies') was stored at −85 °C.

Purity of solubilized UCP1 inclusion bodies

Solubilized UCP1 inclusion bodies were subjected to electrophoresis on 19 cm SDS/12% (w/v) polyacrylamide gels for 2 h at 370 V. UCP1 content was assessed with three different stains over a range of protein loadings. For staining with Coomassie Brilliant Blue R250, protein loaded per lane was 2–16 μg. For staining with silver (Bio-Rad) and SYPRO Orange (Bio-Rad), 0.1–1.0 μg of protein was loaded. Gels were dried overnight and then scanned with a Scanmaker 12 USL (Microtek) scanner. Band intensities were quantified with NIH Image, version 1.60 (ftp://zippy.nimh.nih.gov/pub/nih-image). The UCP1 content of inclusion bodies was quantified by comparing the UCP1 signal either with the signal obtained with BSA (Fraction V, assumed 90% pure) or with the total protein signal obtained within the lane. The estimate of the purity of the preparation used to calibrate UCP1 expression in yeast was 53 ± 7% (mean ± S.E.M. for six values; three stains, each calculated two ways) (Figure 1).

Expression of UCP1 in *Saccharomyces cerevisiae*

A *Bam*HI–*Eco*RI PCR fragment containing only the mouse UCP1 coding sequence (accession ID U63419) preceded at the 5′ end by GCC was obtained from Dr G. Pan (Genentech). Cells of the *S. cerevisiae* diploid W303 (a/α) were transformed [30] with one of three different UCP1 expression constructs. pBF307 (modest UCP1 expression) was made by inserting the fragment into the *Bam*HI–*Eco*RI site in the multiple cloning site in pYES2 (Invitrogen). A second construct, pBF320 (higher UCP1 expression), was made by removing the UCP1 coding sequence from pBF307 on a *Bam*HI–*Xba*I fragment and inserting it into the *Bgl*II site of pKV49 [31] by Klenow blunt-end ligation. pBF320 has a stronger promoter and a higher plasmid copy number and thus gives greater levels of UCP1 expression. A third construct, pBF352, was similar to pBF320 but contained a Kozak sequence (ATAATG) [32,33] at the translation initiation site. UCP1 expression was even stronger in these yeast cells. The UCP1 nucleotide sequence was verified in each case.

Precultures of yeast transformed with the pYES2 constructs (pBF307 or pYES2 empty vector) were grown overnight in selective lactate (SL) medium [34] [2% (w/v) L-lactic acid/0.67% yeast nitrogen base (Difco)/0.1% casamino acids (Difco)/0.12% $(NH_4)_2SO_4$/0.1% KH_2PO_4/0.1% glucose/20 mg/l tryptophan/40 mg/l adenine]. Precultures of yeast transformed with pKV49-based vectors (pBF320, pBF352 or pKV empty vector) were grown similarly in modified SL medium, with a leucine dropout amino acid cocktail [the 25-fold concentrated stock consisted of (in g/l) 0.5 adenine, 0.5 histidine, 0.75 tyrosine, 0.75 lysine, 0.5 arginine, 0.5 methionine, 0.75 isoleucine, 0.125 phenylalanine, 0.5 proline, 0.375 valine, 0.5 threonine, 0.875 serine, 0.25 glutamate, 0.25 aspartate, 0.5 glycine, 0.5 asparagine, 0.5 alanine, 0.5 cysteine and 0.5 uracil] in place of casamino acids. Precultures of pBF307 or pBF320 yeast were grown to a D_{600} of approx. 2.0, then transferred to a selective galactose medium [34] [2% D-galactose/0.67% yeast nitrogen base/40 mg/l adenine/20 mg/l tryptophan, supplemented with 0.1% casamino acids (ura^-) or with leucine dropout amino acid cocktail and 20 mg/l uracil (leu^-)] for growth and induction of UCP1 expression overnight (approx. 16 h). Precultures of pBF352 yeast were transferred to SL medium without glucose, containing 3% lactate (pH 6) for growth overnight, then induced for 0–4 h with 1% (w/v) galactose.

Isolation of yeast mitochondria

Mitochondria were isolated [35] from yeast cultures with a D_{600} of approx. 1.5. Cells were harvested by centrifugation at 2500 ***g*** for 5 min at room temperature, resuspended in Milli-Q water and re-centrifuged, then resuspended in buffer containing 100 mM Tris/HCl and 20 mM dithiothreitol, pH 9.3, and incubated for 10 min at 30 °C. They were re-centrifuged, washed twice in buffer containing 100 mM Tris/HCl and 500 mM KCl, pH 7.0, and resuspended in 5 ml of isotonic spheroplasting buffer [40 mM citric acid/120 mM Na_2HPO_4/1.35 M sorbitol/1 mM EGTA (pH 5.8)]. Lyticase was added at 3 mg/ml; the cells were incubated at 30 °C for exactly 30 min. Subsequent steps were at 4 °C. Spheroplasts were pelleted, washed twice in 40 ml of buffer containing 10 mM Tris/maleate, 0.75 M sorbitol, 0.4 M man-

nitol, 2 mM EGTA and 0.1 % BSA, pH 6.8, then resuspended in 25 ml of mitochondrial isolation buffer [36] [0.6 M mannitol/10 mM Tris/maleate/0.5 mM Na_2HPO_4/1 % (w/v) BSA (pH 6.8)], with one protease inhibitor tablet (Complete®, Boehringer) added per 40 ml immediately before use. The spheroplasts were homogenized by 12 passes with a Wesley Coe homogenizer. The homogenate was centrifuged at 800 ***g*** for 10 min. The supernatants were removed by pipette, to prevent disruption of the pellet, and centrifuged at 11000 ***g*** for 10 min. Mitochondrial pellets were washed in buffer containing 10 mM Tris/maleate, 0.65 M mannitol and 2 mM EGTA, pH 6.8, then resuspended in a small volume of this buffer and assayed for protein content by the biuret method [37].

Respiration with NADH as substrate

Respiration was measured at 30 °C immediately after mitochondrial isolation. Mitochondria were suspended at 0.15 mg of protein/ml in 2 ml of electrode buffer [10 mM Tris/maleate/0.6 M mannitol/0.5 mM EGTA/2 mM $MgCl_2$/10 mM K_2HPO_4/0.1 % BSA (pH 6.8)] containing 3 mM NADH in a Rank oxygen electrode. Respiratory control ratios (rate with FCCP divided by rate without) for control mitochondria were approx. 7 (see Table 2), which were comparable with published values [2,13,15].

Proton conductance

Ascorbate (2 mM) in the presence of the artificial electron carrier *N*,*N*,*N*′,*N*′-tetramethyl-*p*-phenylenediamine (TMPD) was used as a well-defined respiratory substrate whose oxidation could be titrated conveniently. Ascorbate oxidation is via cytochrome oxidase and is linearly dependent on TMPD, which is required for the catalysis of electron transport to mitochondrial cytochrome *c*.

The oxygen electrode was fitted with a methyltriphenylphosphonium (TPMP)-sensitive electrode to allow simultaneous measurements of membrane potential [38] and oxygen consumption rate (which is equal to proton leak rate divided by the H/O ratio of 4.0). The dependence of oxygen consumption rate on membrane potential as substrate oxidation is varied by increasing the concentration of TMPD yields the kinetic response of the proton leak to its driving force. The proton conductance at each membrane potential can be read from the proton leak curves.

Mitochondria were suspended at 0.5 mg of protein/ml in electrode buffer at 30 °C. Oligomycin (1 μg/ml) was added to inhibit the ATP synthase, so that all oxygen consumption was attributable to proton leak and not to ATP synthesis. Nigericin (100 ng/ml) was added to clamp the pH gradient across the mitochondrial membrane. Myxothiazol (3 μM) was added to inhibit electron transport at respiratory complex III because some additions were in ethanol, which can be oxidized by yeast mitochondria through an NADH-linked pathway. The TPMP electrode was then calibrated with four successive additions each of 1 μM TPMP. Ascorbate oxidation was increased sequentially by adding TMPD to concentrations of 3.125, 6.25, 12.25, 25, 37.5, 50 and 75 μM. At each TMPD concentration, steady-state oxygen consumption and membrane potential were measured. Membrane potentials were calculated from TPMP concentrations outside the mitochondria, as described by Brand [38], assuming a TPMP binding correction of 0.4 $\mu l^{-1} \cdot mg$. A different TPMP binding correction would affect all the measured values of membrane potential equally and would therefore not affect our conclusions. Any differences in TPMP binding between UCP1-containing and control yeast mitochondria would matter; however, the similarity of the proton leak curves with empty vector and with UCP1 plus GDP (see Figure 3) suggests that any such differences are insignificant.

Brown-adipose-tissue mitochondria were isolated as described by Cannon and Lindberg [39] from female Syrian hamsters kept at room temperature and fed *ad libitum*.

All mitochondrial samples were stored at −30 °C for subsequent Western blotting.

Western blots

For determination of UCP1 expression levels in yeast and brown-adipose-tissue mitochondria, samples and solubilized UCP1 inclusion bodies were loaded on an SDS/12 % (w/v) polyacrylamide gel and run at 160 V for 35 min in Tris/glycine running buffer (consisting of 28.8 g/l glycine and 6 g/l Tris base) containing 0.1 % SDS. Protein was transferred to a PVDF membrane by using a Bio-Rad Trans-Blot® SD semi-dry electrophoretic transfer cell at 10 V for 35 min in buffer containing 25 mM 3-(cyclohexylamino)propane-1-sulphonic acid ('Caps'), 20 % (v/v) methanol and 0.05 % SDS. The membrane was blocked for 1 h at room temperature in PBS containing 0.1 % (v/v) Tween 20 and 5 % (w/v) Marvel™ non-fat dry milk powder, exposed overnight at 4 °C to an affinity-purified polyclonal UCP1 antibody (raised to a 19-residue peptide corresponding to the C-terminus of mUCP1; Chemicon) diluted 1:4000 in blocking buffer, washed several times in blocking buffer, then incubated for 45 min at room temperature with an alkaline phosphatase-conjugated secondary (anti-rabbit) antibody (New England Biolabs) diluted 1:4000 in blocking buffer. The membrane was washed twice in blocking buffer and twice in a buffer containing 10 mM Tris/HCl, 10 mM NaCl and 1 mM $MgCl_2$, pH 9.5, then developed with a Phototope®-Star Western blot detection kit (New England Biolabs) and exposed for approx. 15 s to Kodak X-OMAT AR scientific imaging film.

UCP1 expression was quantified similarly in pBF352 yeast and hamster brown-adipose-tissue mitochondria but with a different antibody (Chemicon) that had been raised against residues 145–159 of the mouse UCP1 sequence, which is identical in hamster UCP1. This antibody was also used at a 1:4000 dilution in blocking buffer.

Western blot films were scanned and analysed as above. Band intensity was linearly related to solubilized UCP1 inclusion body protein at loadings of between 1 ng and 5 μg ($r^2 = 0.98$). Amounts of UCP1 in yeast mitochondria, run on the same gel as the standards, were calculated by interpolation.

Calculations of UCP1 activities

For comparison with published studies of UCP1 in yeast, which reported mitochondrial respiration only, we measured UCP1-stimulated respiration as the difference between the fully palmitate-stimulated and the fully GDP-inhibited respiration rates. This measurement ignores differences in mitochondrial protonmotive force between the two conditions. Because respiration is strongly controlled by protonmotive force, it provides only a crude indication of UCP1 activity.

For brown-adipose-tissue mitochondria, both membrane potential and respiration have been measured, permitting calculation of the proton conductance (in nmol of H^+/min per mg of protein per mV) of the inner membrane [40–45] (see Table 3). The proton conductance of UCP1-containing proteoliposomes can also be calculated from published data [46,47]. To facilitate comparisons, published values for proton conductance in mitochondria or liposomes were adjusted to 30 °C, assuming a Q_{10} of

2. The conductance of UCP1 was calculated as the proton conductance without GDP minus that with GDP at a given membrane potential. The conductance is approximately constant at potentials below approx. 100 mV (the 'pseudo-linear' range) [40,41,45], permitting a rough comparison of values at different low potentials in different studies. Alternatively, we compared conductances at 126 mV, a value that is reached or can be approximated in our experiments and in a number of published studies. UCP1 catalytic-centre activities were calculated by dividing the proton conductance of UCP1 in the pseudolinear region or at 126 mV by the UCP1 concentration (see Table 3).

Statistical analyses

Means were compared with Student's *t* test.

Chemicals

Chemicals were from Sigma unless stated otherwise. NADH and GDP were dissolved in water, palmitic acid in ethanol and FCCP in methanol (NADH oxidation) or ethanol (ascorbate/TMPD oxidation).

RESULTS

Expression levels of mUCP1 in yeast

The levels of UCP1 expression in mitochondria from yeast containing mUCP1 and from brown adipose tissue were assessed by Western blotting (Figure 2), with solubilized *E. coli* mUCP1 inclusion bodies (53% pure) for calibration (Table 1). The molecular masses of both inclusion body UCP1 and yeast-expressed UCP1 were approx. 32 kDa, as expected. Approximately 0.9 ± 0.2 μg of UCP1 per mg of mitochondrial protein were expressed from pBF307 (modest UCP1 expression) and 11.1 ± 3.9 μg/mg from pBF320 (higher UCP1 expression). UCP1 expression in pBF352 yeast grown in selective lactate medium and induced with 1% (w/v) galactose for 0–4 h was 0.2 ± 0.1 to 11.6 ± 5.5 μg of UCP1 per mg of mitochondrial protein. Even without galactose induction, a small amount of UCP1 was present in pBF352 mitochondria, indicating 'leaky' expression of the pKV49 vector in the absence of glucose (which is required for the complete inhibition of expression). Even at the highest levels of expression achieved, less UCP1 was present than in hamster brown-adipose-tissue mitochondria. The level in hamster brown-adipose-tissue mitochondria was 25 μg/mg of protein (Table 1), comparable with published values (see Table 3).

Yeast transformed with pBF307 (modest UCP1 expression)

Expression of UCP1 in yeast transformed with pBF307 (modest UCP1 expression) had no effect on yeast growth. The mean doubling time after induction with galactose was 1.76 ± 0.14 h, in comparison with 1.82 ± 0.03 h for control cells transformed with empty vector ($P = 0.88$).

In isolated yeast mitochondria oxidizing NADH, there was no effect of modest UCP1 expression on the rate of uncoupled respiration with FCCP present (Table 2). In the presence of GDP, the respiratory control ratio and the non-phosphorylating respiration rate were unchanged. However, in the absence of GDP, non-phosphorylating respiration rates were higher than in empty-vector controls (Table 2). They were stimulated to a greater extent than controls by 100 μM palmitate; this effect was abolished by the addition of GDP. Higher palmitate concentrations (results not shown) increased the GDP-insensitive rates but not the UCP1-specific, GDP-sensitive rates. Respiration due

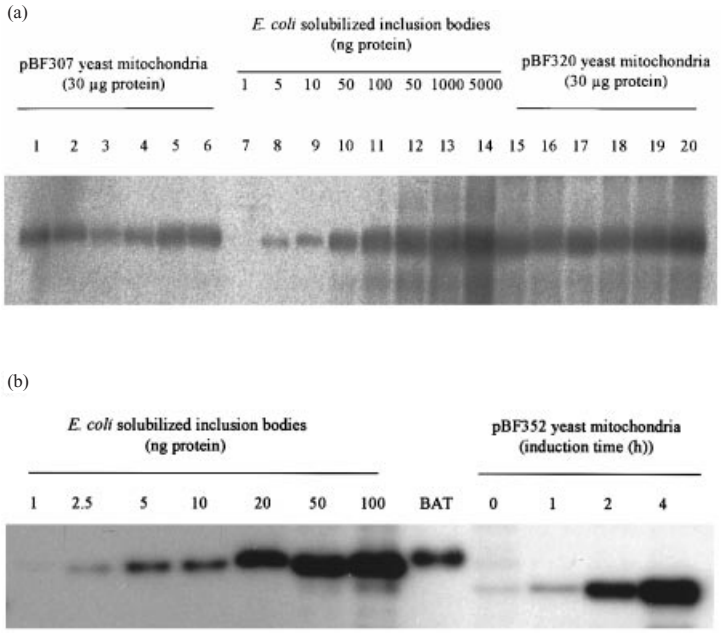

Figure 2 Expression of UCP1 in yeast

(**a**) Western blot showing UCP1 expression levels in yeast mitochondria, calibrated with solubilized UCP1 inclusion bodies isolated from pET-UCP1-transfected *E. coli*. Lanes 1–6, mitochondria (30 μg of protein) from different preparations of yeast containing pBF307 (modest UCP1 expressers); lanes 15–20, mitochondria (30 μg of protein) from different preparations of yeast containing pBF320 (higher UCP1 expressers); lanes 7–14, solubilized UCP1 inclusion bodies isolated from *E. coli* loaded at 1–5000 ng of protein. (**b**) Western blot showing UCP1 expression levels in mitochondria isolated from pBF352 yeast, and in brown-adipose-tissue mitochondria from warm-adapted hamsters. Hamster brown-adipose-tissue mitochondria (BAT) were loaded at 250 ng of mitochondrial protein. Mitochondria from pBF352 yeast were loaded at 10 μg (0, 1 and 2 h of induction) or 5 μg (4 h of induction).

Table 1 UCP1 expression levels determined by Western blotting with UCP1 inclusion bodies in mitochondria isolated from yeast UCP1 expression constructs and from hamster brown adipose tissue

Values are means ± S.E.M. for four to six independent measurements.

Source of mitochondria	Induction conditions	UCP1 content (μg/mg of mitochondrial protein)
pBF307	Overnight 2% galactose	0.9 ± 0.2
pBF320	Overnight 2% galactose	11.1 ± 3.9
pBF352	0 h, 1% galactose	0.2 ± 0.1
pBF352	1 h, 1% galactose	0.3 ± 0.1
pBF352	2 h, 1% galactose	1.6 ± 0.6
pBF352	4 h, 1% galactose	11.6 ± 5.5
Hamster brown adipose tissue	Kept at room temperature (20–25 °C)	24.3 ± 2.2

to UCP1 activity, measured as the difference between the rate of NADH oxidation with palmitate and the rate with palmitate and GDP, was 305 nmol of O/min per mg of mitochondrial protein.

The kinetics of the proton leak (with ascorbate plus TMPD as respiratory substrate) in mitochondria isolated from yeast transformed with pBF307 (modest UCP1 expression) or with empty vector are shown in Figure 3(a). The proton leak had typical non-ohmic kinetics, with proton conductance increasing strongly at higher membrane potentials. In the absence of GDP, mitochondria from yeast expressing modest levels of UCP1 had greater proton conductance than those from empty-vector controls. This is visible in Figure 3(a) as an upward deflection of the curve, with higher rates of oxygen consumption (and therefore of proton leak) at any given membrane potential. The increased proton conductance caused by modest UCP1 expression was completely sensitive to GDP, which returned the kinetics to the basal level seen with empty vector. Proton conductance was calculated for each experimental condition at 137 mV, the lowest common membrane potential. Endogenous proton conductance was 1.5 nmol of H^+/min per mg of protein per mV. With modest UCP1 expression, the extra (GDP-sensitive) proton conductance in the absence of palmitate was 0.5 nmol of H^+/min per mg of protein per mV. When this value is divided by the measured concentration of UCP1 (0.9 μg/mg of protein, or 14 pmol of UCP1 dimer/mg of protein) we obtain a catalytic-centre activity for GDP-sensitive UCP1 proton conductance with no added palmitate of 37 H^+/min per mV. At 126 mV the GDP-sensitive proton conductance was 1.0 nmol of H^+/min per mg of protein per mV and the catalytic-centre activity was 71 H^+/min per mV (Table 3).

The low concentration of palmitate used here (50 μM, in the presence of 0.1% BSA) had a small stimulatory effect on basal proton conductance even in yeast mitochondria containing no UCP1, increasing it from 1.5 to 1.8 nmol of H^+/min per mg of protein per mV in the pseudolinear region. However, the effect was much more pronounced in mitochondria expressing modest levels of UCP1 (Figure 3a). The proton conductance through UCP1 in the presence of palmitate was 1.5 nmol of H^+/min per mg of protein per mV in the pseudolinear region, giving a catalytic-centre activity of 110 H^+/min per mV for UCP1 in the presence of saturating palmitate. At 126 mV the palmitate-stimulated UCP1 proton conductance was 4.1 nmol of H^+/min per mg of protein per mV and the catalytic-centre activity was 290 H^+/min per mV (Table 3).

Yeast transformed with pBF320 (higher UCP1 expression)

Expression of UCP1 in yeast transformed with pBF320 (higher UCP1 expression) caused significant inhibition of growth ($P = 0.027$). The mean doubling time after induction with galactose was 1.99 ± 0.04 h, in comparison with 1.85 ± 0.04 h for empty-vector controls.

Mitochondria from these cells had higher rates of non-phosphorylating respiration with NADH as substrate than controls (Table 2). However, with FCCP present, uncoupled rates were slower than controls. The respiratory control ratio was decreased in the absence and in the presence of GDP. Respiration rates were stimulated to a greater extent than controls by 100 μM palmitate; this effect was abolished by the addition of GDP. Respiration due to UCP1 activity, measured as the difference between the rate of NADH oxidation with palmitate and the rate with palmitate and GDP, was 411 nmol of O/min per mg of mitochondrial protein (Table 2).

In the presence of palmitate, or in the absence of GDP, membrane potential (with ascorbate plus TMPD as respiratory substrate) was small and difficult to measure accurately in mitochondria from cells transformed with pBF320 (higher UCP1 expression). In the presence of 0.5 mM GDP, membrane potential was measurable, allowing the kinetics of the proton leak to be determined (Figure 3b). Increasing the GDP concentration above 0.5 mM had no effect. Even in the presence of saturating GDP concentrations that fully inhibit native UCP1, proton conductance was considerably higher than in empty-vector controls. A significant inhibition of substrate oxidation was again evident, because the maximum non-phosphorylating respiration rate was slower even though the mitochondria had greater background uncoupling with higher UCP1 expression. The artifactual GDP-insensitive proton conductance caused by higher UCP1 expression was approx. 1 nmol of H^+/min per mg of protein per mV at 126 mV; nearly double the basal conductance and as great as the native GDP-sensitive proton conductance in pBF307, showing that the artifactual conductance can easily approach the native conductance under inappropriate expression conditions.

Yeast transformed with pBF352 (highest UCP1 expression)

Expression of UCP1 in pBF352 yeast caused a severe inhibition of growth. To obtain sufficient material for mitochondrial isolation and characterization, these yeast cells were grown in selective lactate medium and UCP1 expression was induced, at a higher D_{600} and for shorter periods, with 1% (w/v) galactose. The mean doubling time after induction under these conditions was 9.6 ± 0.6 h in pBF352 yeast, in comparison with 2.6 ± 0.1 h in paired empty-vector controls ($n = 7$; significantly different, $P < 0.001$).

In mitochondria isolated from these yeast cells, both GDP-sensitive and GDP-insensitive components of proton conductance were apparent. The palmitate-stimulated, GDP-inhibited

Table 2 Non-phosphorylating respiration rates of mitochondria isolated from yeast containing pBF307 (modest UCP1 expression) or pBF320 (higher UCP1 expression), and their paired controls (pYES2 empty vector and pKV empty vector respectively)

BSA was present throughout (see the Experimental section for assay conditions). Values are means ± S.E.M. (n = 5–8). NADH was added as respiratory substrate at 3 mM, GDP at 0.5 mM and palmitate at 100 μM. In several experiments, rates were measured after the addition of NADH and again after the addition of GDP. In all other experiments, rates were measured after addition of NADH and after successive additions of palmitate, then GDP, then carbonyl cyanide p-trifluoromethoxyphenylhydrazone (FCCP). UCP1-dependent respiration was calculated as the difference between the rate with palmitate (fully stimulated) and the rate with palmitate plus GDP (fully inhibited). *Significantly different from paired control ($P < 0.05$); **significantly different from pBF307. Abbreviation: RCR, respiratory control ratio [FCCP-uncoupled rate divided by rate with NADH (or NADH + GDP)].

	Respiration rate (nmol of O/min per mg of mitochondrial protein)						
Yeast strain	NADH	NADH + GDP	NADH + palmitate	NADH + palmitate + GDP	NADH + palmitate + GDP + FCCP	UCP1-dependent respiration	RCR (no GDP)	RCR (+ GDP)
PYES2 empty vector	170 ± 9	170 ± 9	358 ± 37	362 ± 37	1203 ± 96	–	7.1 ± 0.5	7.1 ± 0.5
pBF307 (modest UCP1)	196 ± 13*	173 ± 17	665 ± 131*	360 ± 79	1209 ± 136	305 ± 48	6.1 ± 0.6*	7.4 ± 0.4
PKV49 empty vector	234 ± 27	234 ± 27	604 ± 130	604 ± 130	1666 ± 181	–	7.1 ± 0.2	7.1 ± 0.2
pBF320 (higher UCP1)	363 ± 28*	302 ± 23*	982 ± 11.8*	571 ± 94	1103 ± 140*	411 ± 28**	2.9 ± 0.3*	3.8 ± 0.4*

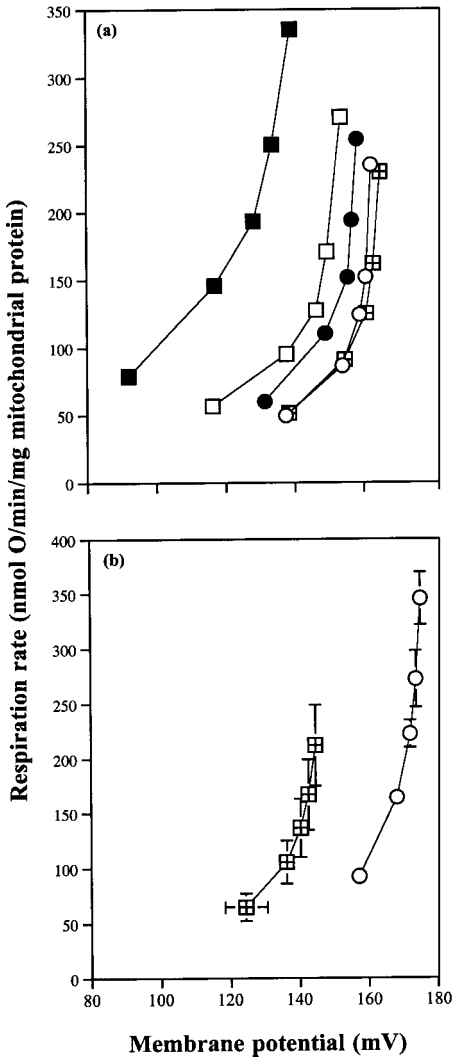

Figure 3 Kinetics of proton leak in mitochondria from yeast expressing mouse UCP1

Oxygen consumption and mitochondrial membrane potential were varied by titration with TMPD in the presence of ascorbate (see the Experimental section). (**a**) Mitochondria were isolated from yeast containing pBF307 (modest UCP1 expression) and from paired controls (yeast containing pYES2 empty vector grown under identical conditions). Where indicated, palmitate was present at 50 μM, or GDP at 0.5 mM. Points represent means from five independent experiments. Error bars have been omitted for clarity but were typically slightly smaller than in (**b**). Symbols: ○, control; ●, control plus palmitate; □, UCP1; ⊞, UCP1 plus GDP; ■, UCP1 plus palmitate. (b) Mitochondria isolated from yeast containing pBF320 (⊞, higher UCP1 expression, in the presence of 0.5 mM GDP) and from paired controls (○, yeast containing pKV-empty vector grown under identical conditions). Results are means ± S.E.M. of three experiments. The differences between control curves in (**a**) and (**b**) might reflect differences in growth conditions (see the Experimental section).

proton conductance was increased from 0 to 4 h of induction (results not shown), demonstrating that the amount of active UCP1 present in mitochondria of pBF352 yeast increased with length of induction. However, the GDP-insensitive proton leak also increased as the duration of induction increased (Figure 4), indicating that mitochondrial integrity became progressively compromised at higher levels of UCP1 expression.

The GDP-sensitive proton conductance attributable to UCP1 activity could not be measured at 126 mV, because this value was not reached in palmitate-stimulated mitochondria from pBF352

Table 3 UCP1 content and catalytic activity in different systems calculated from published data

References are available on request from the authors. Nomenclature: fatty acids low, studies with BSA present or with no added fatty acids; fatty acids higher, studies with fatty acids added; linear region, calculated by using a low potential, assuming ohmic proton conductance.

	Acclimation temperature (°C)	Number of published studies of UCP1 content	Average UCP1 content*		UCPI proton conductance (nmol H^+/min per mg of mitochondrial protein per mV)†				Dimer catalytic-centre activity ($min^{-1} \cdot mV^{-1}$)‡				
					Fatty acids low		Fatty acids higher		Fatty acids low		Fatty acids higher		
			(μg/mg protein)	(pmol of dimer/mg of protein)	Linear region	126 mV	Linear region	126 mV	Linear region	126 mV	Linear region	126 mV	References
Mitochondria isolated from thermoneutral rodents													
Guinea pig	28–32	2	5.5	87									
Hamster	30	3	30	474									
Mouse	28–31	3	6.3	98									
Rat	28–33	22	13	209	0.45	0.52			2.1	2.5			[42–44]
Mean thermoneutral rodent			14	217									
Mitochondria isolated from cold-acclimated rodents													
Guinea-pig	4–8	5	31	488	26				53				[41,45]
Hamster	4–7	18	54	841	15		81		18		96		[40]
Mouse	4–10	8	55	862									
Rat	4–5	39	56	875	3.8	11			4.4	12			[42–44]
Mean cold-acclimated rodent			49	767					25				
Mitochondria isolated from transgenic yeast													
Rat UCP1 in yeast			85	1328									[47]
Rat UCP1 in yeast			24	170									[36]
Hamster UCP1in yeast			24	371									[58,59]
Mouse UCP1 in yeast (pBF307)			0.9	14	0.51	0.99	1.5	4.1	37	71	110	290	This study
Mouse UCP1 in yeast (pBF320)			11	173									This study
Mouse UCP1 in yeast (pBF352)			12	188			5.3				28		This study
Proteoliposomes													
Rat UCP1 in liposomes								24				1.6	[47]
Hamster UCP1 in liposomes					11	11			1.1	1.1			[46]
Hamster UCP1 in liposomes					76	140			8.1	15			[49]

* Average of literature values using GDP binding or UCP1 antibodies, calculated as μg/mg or as pmol of dimer/mg, assuming a dimer molecular mass of 64 kDa.

† GDP-sensitive proton conductance. Values in [45] are corrected to $H^+/O = 6$ for glycerol phosphate oxidation; all values are corrected to 30 °C assuming a Q_{10} of 2.0 for proton conductance.

‡ Calculated from proton conductance using average values of UCP1 content given here (or values for UCP1 purity in the relevant paper, for liposome data).

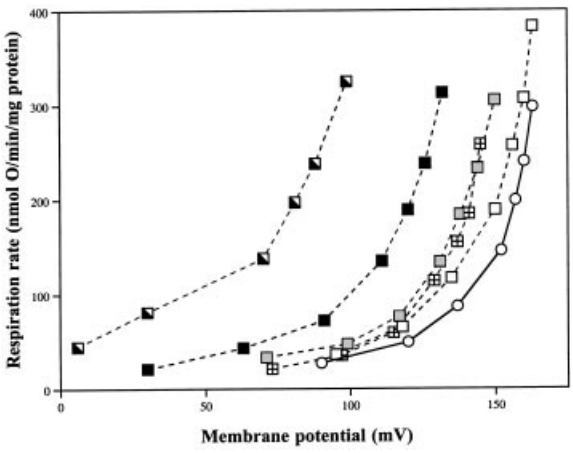

Figure 4 GDP-sensitive and GDP-insensitive proton conductance in mitochondria from pBF352 yeast and paired empty-vector controls

Yeast (pBF352 or empty vector) were induced for 0–4 h before the isolation of mitochondria. For pBF352 mitochondria, individual points are means for three separate experiments. For empty-vector controls, individual points represent pooled data from 12 experiments. In each case, 50 μM palmitate and, except where indicated, 1 mM GDP was present. Error bars have been omitted for clarity; they were similar in magnitude to those in Figure 3(b). Symbols: ○, controls; □, UCP1, 0 h; ⊞ UCP1, 1 h; ▨ UCP1, 2 h; ■, UCP1, 4 h; ◪, UCP1, 4 h (no GDP).

yeast. However, UCP1-mediated proton conductance was calculated in the pseudolinear region (Table 3).

DISCUSSION

Uncoupling of mitochondrial oxidative phosphorylation after the heterologous expression of mammalian uncoupling proteins in yeast has been used to test the proposed native proton-conducting function of the UCP1 homologues. However, there is a danger of false positives in such experiments, therefore making a good control essential. UCP1 is the protein most closely related to UCP2 and UCP3; it provides such a control. Native UCP1 uncoupling activity in mammalian mitochondria is abolished by GDP, so sensitivity to GDP in heterologous expression systems can be used to distinguish between proton conductance mediated by native UCP1 activity and proton conductance occurring through other means. UCP1 therefore provides a better control than less related proteins such as the adenine nucleotide translocase or the oxoglutarate carrier, which have sometimes been used by others. We have shown that increased proton conductance can indeed occur as an artifact of UCP1 expression in yeast. Whereas with modest expression UCP1 showed native behaviour, with higher expression a second, non-native proton leak appeared. This non-native (GDP-insensitive) proton conductance might compromise the interpretation of experiments in which UCP1 homologues are expressed in yeast and other systems. Indeed, we have observed that the proton conductance caused by the expression of UCP2 and UCP3 in yeast is only seen at supraphysiological amounts of these proteins ([47a], and J. A. Harper, J. A. Stuart, M. B. Jekabsons, K. M. Brindle and M. D. Brand, unpublished work).

Yeast as a model system for studying UCP1 function

The levels of UCP1 protein in our yeast expression constructs were quantified and compared with levels found in hamster brown-adipose-tissue mitochondria (Table 1). For comparison, Table 3 lists levels of mammalian UCP1 observed by others in brown adipose tissue and in transformed yeast mitochondria.

Expression levels in brown-adipose-tissue mitochondria from animals kept at thermoneutral temperatures range from 6 μg/mg of protein in guinea-pig and mouse to 30 in hamster, with an average of 14 μg/mg. Our yeast expressing modest amounts of mouse UCP1 (0.9 μg/mg of mitochondrial protein) therefore expresses mUCP1 at 15% of the amount in thermoneutral mouse brown-adipose-tissue mitochondria or 6% of the mean level in rodents. Our higher expresser (11 μg/mg) expresses mUCP1 at almost twice the level in thermoneutral mouse brown-adipose-tissue mitochondria or 80% of the mean level in rodents. Expression levels in brown-adipose-tissue mitochondria from animals kept in the cold range from 31 μg/mg of protein in guinea-pig to 56 μg/mg in rat or mouse, with an average of 49 μg/mg. Our higher expresser therefore expresses mUCP1 at 35% of the level in cold-adapted guinea-pig or 22% of the mean level in cold-adapted rodents.

Table 3 lists proton conductances and H^+ catalytic-centre activities for UCP1 for isolated mammalian mitochondria and for UCP1 incorporated into proteoliposomes, calculated by us from published data. There are no values for yeast mitochondria expressing mammalian UCP1, because mitochondrial membrane potential was not reported in the published studies. Catalytic-centre activities describe the catalytic activity of a protein, and so can be used to compare the quality of different preparations and expression systems. Early work at low potential [40,41,46,48] suggested that the proton conductance of UCP1 is ohmic (constant conductance). However, it is now clear that it is non-ohmic at higher membrane potentials and that the proton conductance of UCP1 increases markedly as membrane potential rises [42–44,49]; this is also apparent in Figures 3 and 4. The catalytic-centre activity therefore varies with potential and, unlike a conventional enzyme, does not tend towards a saturating value.

The calculated catalytic-centre activity of UCP1 dimers in brown-adipose-tissue mitochondria from cold-adapted animals in the pseudolinear region varied from 4 to 53 $H^+ \cdot min^{-1} \cdot mV^{-1}$, with an average value of 25 $min^{-1} \cdot mV^{-1}$ (Table 3). The catalytic-centre activity for our modest UCP1 expresser was 37 $min^{-1} \cdot mV^{-1}$, suggesting near-native activity of mammalian UCP1 in this heterologous yeast expression system despite differences in phospholipids and other membrane proteins. All of these values are for mitochondria at 30 °C. Because they were incubated in BSA without fatty acids, which are important or even essential cofactors [50,51], they underestimate the true catalytic activity of UCP1. With BSA absent, a minimum estimate of the catalytic-centre activity in hamster brown adipose tissue is 96 $min^{-1} \cdot mV^{-1}$ [52,53], comparable with our value for yeast of 110 with added palmitate. The pattern at 126 mV is similar (Table 3). Our catalytic-centre activity of 290 $min^{-1} \cdot mV^{-1}$ for UCP1 in yeast at 126 mV is the first value reported at higher potential with palmitate present and suggests the catalytic activity of UCP1 under more plausibly physiological conditions. The catalytic-centre activities that we calculate for UCP1 incorporated into proteoliposomes are rather lower than the values in mitochondria, suggesting that these purified and reconstituted systems are not always fully active and therefore that they might not always display the native properties of UCP1. Indeed, there is evidence that an essential cofactor for UCP1 activity might be absent from liposome model systems in which UCP1 has been purified from a bacterial source [54].

In our experiments, uncoupling resulting from modest UCP1 expression in pBF307 yeast was completely GDP-sensitive. In

the presence of GDP, the respiratory characteristics and proton leak kinetics of these mitochondria were indistinguishable from empty-vector controls. These observations suggest that induction of expression in pBF307 leads to native-like UCP1 function in the mitochondrial membrane and we conclude that modest expression of UCP1 in yeast is a good experimental model for studying mammalian UCP1 function.

Artifactual uncoupling with stronger induction of UCP1 expression

Although expression in pBF307 resulted in apparently native behaviour of UCP1, this was not so at the higher levels of expression achieved in pBF320 and pBF352. In these experiments, with up to 12-fold more UCP1, there was an increase in non-phosphorylating respiration in comparison with the modest expressers (Table 2). However, there was also evidence of mitochondrial dysfunction that was not attributable to native UCP1 activity. Two experimental artifacts were observed in high expressers: (1) the higher mitochondrial proton conductance could not be completely abolished by GDP [this can be seen both in the proton leak kinetics (Figures 3b and 4) and in respiration (Table 2)], and (2) substrate oxidation was compromised [this is particularly obvious in Figure 3(b), where, at each concentration of TMPD, oxygen consumption was lower in UCP1 mitochondria, despite membrane potential also being lower; it can also be seen in Table 2, where mitochondria expressing high levels of UCP1 had significantly lower FCCP-uncoupled rates of NADH oxidation than paired controls]. A similar inhibition of substrate oxidation is evident in other experiments in which UCP1 homologues have been expressed heterologously or transgenically [14,15,17].

UCP1 H^+ turnover in pBF352 yeast mitochondria was calculated in the pseudolinear region for comparison with other published values (see Table 3) or at 100 mV, for comparison with mitochondria from pBF307 yeast. The proton leak attributable to palmitate-stimulated UCP1 activity was 79 nmol of H^+/min per μg of UCP1 in pBF352 and 378 nmol of H^+/min per μg of UCP1 in pBF307. Therefore the specific activity of UCP1 expressed in pBF352 was approx. 20% of that in pBF307. This illustrates clearly that, under the stronger conditions of expression, either a significant proportion of the protein was inactive, or perhaps all of the synthesized protein was submaximally active.

The UCP1 concentration in our high expressers, which showed artifactual proton conductance, was lower than those reported in two other studies. Arechaga et al. [36] expressed UCP1 at 24 μg/mg of mitochondrial protein in the same strain of yeast. Under virtually identical experimental conditions, the UCP1-stimulated respiration rate was approx. 280 nmol of O/min per mg of mitochondrial protein [36], in comparison with approx. 305 nmol of O/min per mg in mitochondria from our yeast transformed with pBF307 (modest UCP1 expression), despite a 25-fold higher UCP1 expression in Arechaga et al. [36]. This might indicate that some UCP1 in the mitochondrial fraction in [36] was inactive. The authors do not state whether UCP1 expression altered fully uncoupled respiration rates. However, when GDP was present to inhibit native UCP1 activity, respiration rates of UCP1-expressing mitochondria were apparently more than double those of controls (Figure 5 of [36]), suggesting that some artifactual uncoupling was present.

Murdza-Inglis et al. [47] also report expression of higher amounts of UCP1 in yeast mitochondria: 70–100 μg of UCP1 per mg of mitochondrial protein (although results are not shown). However, the UCP1-stimulated respiration rate that can be calculated from this study is notably low, approx. 96 nmol of O/min per mg of mitochondrial protein, suggesting that much of the UCP1 in the mitochondria in [47] is not active. Similarly, the catalytic-centre activity for UCP1 incorporated into liposomes in [47] can be estimated to be less than 2 $min^{-1} \cdot mV^{-1}$ at 126 mV. Comparison with the value of 290 $min^{-1} \cdot mV^{-1}$ for GDP-sensitive UCP1 in yeast mitochondria under comparable conditions (Table 3) suggests that most of the UCP1 in this reconstituted liposome system lacks native activity. Despite these artifacts, the conclusions relating to the native activities that were measured in [36,47] should remain valid.

The expression artifacts seen in the present study occur at lower UCP1 expression levels than those in cold-adapted brown-adipose-tissue mitochondria (see Table 3). It is possible that the amount of protein inserted into yeast mitochondria is less important than the rate of UCP1 expression. Brown-adipose-tissue mitochondria might take days to increase UCP1 content severalfold during adaptation to cold; in the yeast expression systems similar amounts are expressed in a few hours. Indeed, in the most strongly expressing plasmid, pBF352, there is some evidence of a GDP-insensitive proton conductance even at 1 and 2 h of induction, when UCP1 protein levels are only approx. 0.3 μg/mg of protein. This suggests that the appearance of the proton leak and substrate oxidation inhibition artifacts was at least in part a function of the rate of UCP1 synthesis, and not simply the amount.

Also, it might be more appropriate to consider UCP1 expression per unit of inner membrane surface area rather than per mg of total mitochondrial protein. Brown-adipose-tissue mitochondria have a notably high cristal density, which increases severalfold in cold acclimation [55]. In contrast, the cristal density of yeast mitochondria grown on respiratory substrate [56] is similar to that of mammalian liver mitochondria [57], and appreciably lower than in brown-adipose-tissue mitochondria. Thus the insertion of UCP1 into yeast mitochondrial inner membranes at the concentrations of UCP1 per mg of mitochondrial protein found in brown-adipose-tissue mitochondria might result in much higher levels of UCP1 per unit membrane surface area in yeast. This could compromise the function of the already densely packed inner membrane.

In conclusion, our results indicate that an artifactual increase in mitochondrial proton conductance can occur under some conditions of UCP1 expression in yeast. The fact that the expression artifact seems to be very similar to the increased proton conductance observed after expression of the UCP1 homologues in yeast should be considered when assessing the functions of these proteins.

We thank Mike Runswick for help with the expression of UCP1 in *E. coli*. The laboratory of M. D. B. is funded by the Medical Research Council. J. A. S., M. D. B. and K. M. B. received support from Wellcome Trust grant 052564/Z/97/Z/BS/LW. J. A. H. was supported by a BBSRC/CASE studentship and by Knoll Pharmaceuticals. M. B. J. was supported by Knoll Pharmaceuticals.

REFERENCES

1 Cannon, B., Matthias, A., Golozoubova, V., Ohlson, K. B. E., Andersson, U., Jacobsson, A. and Nedergaard, J. (1999) Unifying and distinguishing features of brown and white adipose tissues: UCP1 versus other UCPs. In Progress in Obesity Research, vol. 8 (Ailhaud, G. and Guy-Grand, B., eds), pp. 13–26, John Libbey & Co. Ltd

2 Fleury, C., Neverova, M., Collins, S., Raimbault, S., Champigny, O., Levi-Meyrueis, C., Bouillaud, F., Seldin, M. F., Surwit, R. S., Ricquier, D. and Warden, C. H. (1997) Uncoupling protein-2: a novel gene linked to obesity and hyperinsulinemia. Nat. Genet. **15**, 269–272

3 Boss, O., Samec, S., Paoloni-Giacobino, A., Rossier, C., Dulloo, A., Seydoux, J., Muzzin, P. and Giacobino, J. P. (1997) Uncoupling protein-3: a new member of the mitochondrial carrier family with tissue-specific expression. FEBS Lett. **408**, 39–42

4 Gimeno, R. E., Dembski, M., Weng, X., Deng, N., Shyjan, A. W., Gimeno, C. J., Iris, F., Ellis, S. J., Woolf, E. A. and Tartaglia, L. A. (1997) Cloning and characterization of an uncoupling protein homolog: a potential molecular mediator of human thermogenesis. Diabetes **46**, 900–906

5 Vercesi, A. E., Martins, I. S., Silva, M. A. P., Leite, H. M. F., Cuccovia, I. M. and Chalmovich, H. (1995) Pumping plants. Nature (London) **375**, 24

6 Laloi, M., Klein, M., Riesmeier, J. W., Muller-Rober, B., Fleury, C., Bouillaud, F. and Ricquier, D. (1997) A plant cold-induced uncoupling protein. Nature (London) **389**, 135–136

7 Mao, W., Yu, X. X., Zhong, A., Li, W., Brush, J., Sherwood, S. W., Adams, S. H. and Pan, G. (1999) UCP4, a novel brain-specific mitochondrial protein that reduces membrane potential in mammalian cells. FEBS Lett. **443**, 326–330

8 Sanchis, D., Fleury, C., Chomiki, N., Goubern, M., Huang, Q., Neverova, M., Gregoire, F., Easlick, J., Raimbault, S., Levi-Meyrueis, C. et al. (1998) BMCP1, a novel mitochondrial carrier with high expression in the central nervous system of humans and rodents, and respiration uncoupling activity in recombinant yeast. J. Biol. Chem. **273**, 34611–34615

9 Brand, M. D., Brindle, K. M., Buckingham, J. A., Harper, J. A., Rolfe, D. F. S. and Stuart, J. A. (1999) The significance and mechanism of mitochondrial proton conductance. Int. J. Obes. **23** (Suppl. 6), S4–S11

10 Stuart, J. A., Brindle, K. M., Harper, J. A. and Brand, M. D. (1999) Mitochondrial proton leak and the uncoupling proteins. J. Bioenerg. Biomembr. **31**, 517–525

11 Stuart, J. A., Cadenas, S., Jekabsons, M. B., Roussel, D. and Brand, M. D. (2001) Mitochondrial proton leak and the uncoupling protein 1 homologues. Biochim. Biophys. Acta **1504**, 144–158

12 Hinz, W., Faller, B., Gruninger, S., Gazzotti, P. and Chiesi, M. (1999) Recombinant human uncoupling protein-3 increases thermogenesis in yeast cells. FEBS Lett. **448**, 57–61

13 Hinz, W., Gruninger, S., De Pover, A. and Chiesi, M. (1999) Properties of the human long and short isoforms of the uncoupling protein-3 expressed in yeast cells. FEBS Lett. **462**, 411–415

14 Zhang, C. Y., Hagen, T., Mootha, V. K., Slieker, L. J. and Lowell, B. B. (1999) Assessment of uncoupling activity of uncoupling protein 3 using a yeast heterologous expression system. FEBS Lett. **449**, 129–134

15 Rial, E., Gonzalez-Barroso, M., Fleury, C., Iturrizaga, S., Sanchis, D., Jimenez-Jimenez, J., Ricquier, D., Goubern, M. and Bouillaud, F. (1999) Retinoids activate proton transport by the uncoupling proteins UCP1 and UCP2. EMBO J. **18**, 5827–5833

16 Clapham, J. C., Arch, J. R., Chapman, H., Haynes, A., Lister, C., Moore, G. B., Piercy, V., Carter, S. A., Lehner, I., Smith, S. A. et al. (2000) Mice overexpressing human uncoupling protein-3 in skeletal muscle are hyperphagic and lean. Nature (London) **406**, 415–418

17 Cadenas, S., Buckingham, J. A., Clapham, J. C. and Brand, M. D. (2000) Human uncoupling protein-3 overexpression increases mitochondrial proton leak. Int. J. Obes. **24** (Suppl. 1), S187

18 Gong, D. W., Monemdjou, S., Gavrilova, O., Leon, L. R., Marcus-Samuels, B., Chou, C. J., Everett, C., Kozak, L. P., Li, C., Deng, C. et al. (2000) Lack of obesity and normal response to fasting and thyroid hormone in mice lacking uncoupling protein-3. J. Biol. Chem. **275**, 16251–16257

19 Vidal-Puig, A. J., Grujic, D., Zhang, C. Y., Hagen, T., Boss, O., Ido, Y., Szczepanik, A., Wade, J., Mootha, V., Cortright, R. et al. (2000) Energy metabolism in uncoupling protein 3 gene knockout mice. J. Biol. Chem. **275**, 16258–16266

20 Jaburek, M., Varecha, M., Gimeno, R. E., Dembski, M., Jezek, P., Zhang, M., Burn, P., Tartaglia, L. A. and Garlid, K. D. (1999) Transport function and regulation of mitochondrial uncoupling proteins 2 and 3. J. Biol. Chem. **274**, 26003–26007

21 Echtay, K. S., Liu, Q., Caskey, T., Winkler, E., Frischmuth, K., Bienengraber, M. and Klingenberg, M. (1999) Regulation of UCP3 by nucleotides is different from regulation of UCP1. FEBS Lett. **450**, 8–12

22 Samec, S., Seydoux, J. and Dulloo, A. G. (1998) Role of UCP homologues in skeletal muscles and brown adipose tissue: mediators of thermogenesis or regulators of lipids as fuel substrate? FASEB J. **12**, 715–724

23 Cadenas, S., Buckingham, J. A., Samec, S., Seydoux, J., Din, N., Dulloo, A. G. and Brand, M. D. (1999) UCP2 and UCP3 rise in starved rat skeletal muscle but mitochondrial proton conductance is unchanged. FEBS Lett. **462**, 257–260

24 Jekabsons, M. B., Gregoire, F. M., Schonfeld-Warden, N. A., Warden, C. H. and Horwitz, B. A. (1999) T(3) stimulates resting metabolism and UCP-2 and UCP-3 mRNA but not nonphosphorylating mitochondrial respiration in mice. Am. J. Physiol. **277**, E380–E389

25 Lanni, A., Beneduce, L., Lombardi, A., Moreno, M., Boss, O., Muzzin, P., Giacobino, J. P. and Goglia, F. (1999) Expression of uncoupling protein-3 and mitochondrial activity in the transition from hypothyroid to hyperthyroid state in rat skeletal muscle. FEBS Lett. **444**, 250–254

26 Matthias, A., Jacobsson, A., Cannon, B. and Nedergaard, J. (1999) The bioenergetics of brown fat mitochondria from UCP1-ablated mice. Ucp1 is not involved in fatty acid-induced de-energization ('uncoupling'). J. Biol. Chem. **274**, 28150–28160

27 Yu, X. X., Barger, J. L., Boyer, B. B., Brand, M. D., Pan, G. and Adams, S. H. (2000) Impact of endotoxin on UCP homolog mRNA abundance, thermoregulation, and mitochondrial proton leak kinetics. Am. J. Physiol. Endocrinol. Metab. **279**, E433–E446

28 Stuart, J. A., Harper, J. A., Brindle, K. M. and Brand, M. D. (2000) An uncoupling artifact can accompany uncoupling protein-1 expression in yeast mitochondria. Int. J. Obes. **24** (Suppl. 1), S187

29 Way, M., Pope, B., Gooch, J., Hawkins, M. and Weeds, A. G. (1990) Identification of a region in segment 1 of gelsolin critical for actin binding. EMBO J. **9**, 4103–4109

30 Hinnen, A., Hicks, J. B. and Fink, G. R. (1978) Transformation of yeast. Proc. Natl. Acad. Sci. U.S.A. **75**, 1929–1933

31 Bathgate, B., Freebairn, E. M., Greenland, A. J. and Reid, G. A. (1992) Functional expression of the rat brown adipose tissue uncoupling protein in *Saccharomyces cerevisiae*. Mol. Microbiol. **6**, 363–370

32 Kozak, M. (1987) An analysis of 5′-noncoding sequences from 699 vertebrate messenger RNAs. Nucleic Acids Res. **15**, 8125–8148

33 Kozak, M. (1991) An analysis of vertebrate mRNA sequences: intimations of translational control. J. Cell Biol. **115**, 887–903

34 Bouillaud, F., Arechaga, I., Petit, P. X., Raimbault, S., Levi-Meyrueis, C., Casteilla, L., Laurent, M., Rial, E. and Ricquier, D. (1994) A sequence related to a DNA recognition element is essential for the inhibition by nucleotides of proton transport through the mitochondrial uncoupling protein. EMBO J. **13**, 1990–1997

35 Guerin, B., Labbe, P. and Somlo, M. (1979) Preparation of yeast mitochondria (*Saccharomyces cerevisiae*) with good P/O and respiratory control ratios. Methods Enzymol. **55**, 149–159

36 Arechaga, I., Raimbault, S., Prieto, S., Levi-Meyrueis, C., Zaragoza, P., Miroux, B., Ricquier, D., Bouillaud, F. and Rial, E. (1993) Cysteine residues are not essential for uncoupling protein function. Biochem. J. **296**, 693–700

37 Gornall, A. G., Bardawill, C. J. and David, M. M. (1949) Determination of serum protein by means of the biuret reaction. J. Biol. Chem. **177**, 751–766

38 Brand, M. D. (1995) Measurement of mitochondrial protonmotive force. In Bioenergetics, A Practical Approach (Brown, G. C. and Cooper, C. E., eds.), pp. 39–62, IRL Press, Oxford

39 Cannon, B. and Lindberg, O. (1979) Mitochondria from brown adipose tissue: isolation and properties. Methods Enzymol. **55**, 65–78

40 Nicholls, D. G. (1974) Hamster brown-adipose-tissue mitochondria. The control of respiration and the proton electrochemical potential gradient by possible physiological effectors of the proton conductance of the inner membrane. Eur. J. Biochem. **49**, 573–583

41 Nicholls, D. G. and Bernson, V. S. (1977) Inter-relationships between proton electrochemical gradient, adenine-nucleotide phosphorylation potential and respiration, during substrate-level and oxidative phosphorylation by mitochondria from brown adipose tissue of cold-adapted guinea-pigs. Eur. J. Biochem. **75**, 601–612

42 Goubern, M., Yazbeck, J., Chapey, M. F., Diolez, P. and Moreau, F. (1990) Variations in energization parameters and proton conductance induced by cold adaptation and essential fatty acid deficiency in mitochondria of brown adipose tissue in the rat. Biochim. Biophys. Acta **1015**, 334–340

43 Goubern, M., Chapey, M. F. and Portet, R. (1991) Time-course variations of effective proton conductance and GDP binding in brown adipose tissue mitochondria of rats during prolonged cold exposure. Comp. Biochem. Physiol. B **100**, 727–732

44 Goubern, M., Chapey, M. F., Senault, C., Laury, M. C., Yazbeck, J., Miroux, B., Ricquier, D. and Portet, R. (1992) Effect of sympathetic de-activation on thermogenic function and membrane lipid composition in mitochondria of brown adipose tissue. Biochim. Biophys. Acta **1107**, 159–164

45 Nicholls, D. G. (1977) The effective proton conductance of the inner membrane of mitochondria from brown adipose tissue. Dependency on proton electrochemical potential gradient. Eur. J. Biochem. **77**, 349–356

46 Klingenberg, M. and Winkler, E. (1985) The reconstituted uncoupling protein is a membrane-potential driven H^+ translocator. EMBO J. **4**, 3087–3092

47 Murdza-Inglis, D. L., Patel, H. V., Freeman, K. B., Jezek, P., Orosz, D. E. and Garlid, K. D. (1991) Functional reconstitution of rat uncoupling protein following its high level expression in yeast. J. Biol. Chem. **266**, 11871–11875

47a Stuart, J. A., Harper, J. A., Brindle, K. M., Jekabsons, M. B. and Brand, M. D (2001) Physiological levels of mammalian Uncoupling Protein 2 do not uncouple yeast mitochondria. J. Biol. Chem. **276**, in the press

48 Trayhurn, P. and Milner, R. E. (1989) A commentary on the interpretation of in vitro biochemical measures of brown adipose tissue thermogenesis. Can. J. Physiol. Pharmacol. **67**, 811–819

49 Winkler, E. and Klingenberg, M. (1992) An improved procedure for reconstitution of the uncoupling protein and in-depth analysis of H^+/OH^- transport. Eur. J. Biochem. **207**, 135–145 [erratum, Eur. J. Biochem. **209**, 1063]

50 Rial, E., Poustie, A. and Nicholls, D. G. (1983) Brown-adipose-tissue mitochondria: the regulation of the 32000-M_r uncoupling protein by fatty acids and purine nucleotides. Eur. J. Biochem. **137**, 197–203

51 Garlid, K. D., Jaburek, M. and Jezek, P. (1998) The mechanism of proton transport mediated by mitochondrial uncoupling proteins. FEBS Lett. **438**, 10–14
52 Nicholls, D. G. (1976) The bioenergetics of brown adipose tissue mitochondria. FEBS Lett. **61**, 103–110
53 Nicholls, D. G. (1976) Hamster brown-adipose-tissue mitochondria. Purine nucleotide control of the ion conductance of the inner membrane, the nature of the nucleotide binding site. Eur. J. Biochem. **62**, 223–228
54 Echtay, K. S., Winkler, E. W. and Klingenberg, M. (2000) Coenzyme Q is an obligatory cofactor for uncoupling protein function. Nature (London) **408**, 609–613
55 Lindgren, G. and Barnard, T. (1972) Changes in interscapular brown adipose tissue of rat during perinatal and early postnatal development and after cold acclimation. Exp. Cell Res. **70**, 81–90
56 Damsky, C. H. (1976) Environmentally induced changes in mitochondria and endoplasmic reticulum of *Saccharomyces carlsbergensis* yeast. J. Cell Biol. **71**, 123–135
57 Porter, R. K., Hulbert, A. J. and Brand, M. D. (1996) Allometry of mitochondrial proton leak: influence of membrane surface area and fatty acid composition. Am. J. Physiol. **271**, R1550–R1560
58 Echtay, K. S., Bienengraeber, M. and Klingenberg, M. (1997) Mutagenesis of the uncoupling protein of brown adipose tissue. Neutralization of E190 largely abolishes pH control of nucleotide binding. Biochemistry **36**, 8253–8260
59 Echtay, K. S., Bienengraeber, M., Winkler, E. and Klingenberg, M. (1998) In the uncoupling protein (UCP-1) His-214 is involved in the regulation of purine nucleoside triphosphate but not diphosphate binding. J. Biol. Chem. **273**, 24368–24374

Received 14 December 2000/19 February 2001; accepted 5 April 2001